

4-2015

## Locally smeared operator product expansions in scalar field theory

Christopher J. Monahan  
*William & Mary*, [cjmonahan@wm.edu](mailto:cjmonahan@wm.edu)

Kostas Orginos  
*William & Mary*, [kostas@wm.edu](mailto:kostas@wm.edu)

Follow this and additional works at: <https://scholarworks.wm.edu/aspubs>



Part of the [Physics Commons](#)

---

### Recommended Citation

Monahan, Christopher J. and Orginos, Kostas, Locally smeared operator product expansions in scalar field theory (2015). *Physical Review D*, 91(7).  
<https://doi.org/10.1103/PhysRevD.91.074513>

This Article is brought to you for free and open access by the Arts and Sciences at W&M ScholarWorks. It has been accepted for inclusion in Arts & Sciences Articles by an authorized administrator of W&M ScholarWorks. For more information, please contact [scholarworks@wm.edu](mailto:scholarworks@wm.edu).

**Locally smeared operator product expansions in scalar field theory**

Christopher Monahan\*

*Physics Department, College of William and Mary, Williamsburg, Virginia 23187, USA*

Kostas Orginos

*Physics Department, College of William and Mary, Williamsburg, Virginia 23187, USA  
and Thomas Jefferson National Accelerator Facility, Newport News, Virginia 23606, USA*

(Received 27 January 2015; published 20 April 2015)

We propose a new locally smeared operator product expansion to decompose nonlocal operators in terms of a basis of smeared operators. The smeared operator product expansion formally connects nonperturbative matrix elements determined numerically using lattice field theory to matrix elements of nonlocal operators in the continuum. These nonperturbative matrix elements do not suffer from power-divergent mixing on the lattice, which significantly complicates calculations of quantities such as the moments of parton distribution functions, provided the smearing scale is kept fixed in the continuum limit. The presence of this smearing scale complicates the connection to the Wilson coefficients of the standard operator product expansion and requires the construction of a suitable formalism. We demonstrate the feasibility of our approach with examples in real scalar field theory.

DOI: [10.1103/PhysRevD.91.074513](https://doi.org/10.1103/PhysRevD.91.074513)

PACS numbers: 11.15.Ha, 12.38.Gc, 14.20.Dh

**I. INTRODUCTION**

QCD connects hadronic matter to its fundamental constituents, quarks, and gluons. Many aspects of QCD are poorly understood, in spite of four decades of intense experimental and theoretical effort. As part of this effort, deep inelastic scattering (DIS) of leptons from nucleons has played a central role in establishing QCD as the reigning theory of the strong interaction and continues to serve as a mainstay for attempts to unravel QCD's mysteries (for complete reviews see, for example, Refs. [1] and [2]).

Theoretically, inclusive DIS cross sections are separated into leptonic and hadronic tensors, which capture the electroweak and strong dynamics of the scattering process, respectively. The hadronic tensor factorizes into a convolution of infrared-safe perturbative coefficients and parton distribution functions (PDFs), which incorporate the low-energy QCD physics and therefore must be determined nonperturbatively. PDFs are independent of the scattering process but depend on the target nucleon, while the perturbative coefficients are independent of the external scattering states.

PDFs are important for two reasons. First, they furnish direct knowledge of the constituents of hadronic states—the dominant form of visible matter in the Universe—in terms of the fundamental theory of the strong force. Second, they provide constraints on hadronic backgrounds at collider experiments, such as the Large Hadron Collider. These backgrounds affect the sensitivity of a variety of high energy experiments, including studies of the properties of

the Higgs boson [3–5] and searches for heavy  $W'$  and  $Z'$  boson production [6].

PDFs cannot currently be calculated directly from QCD using *ab initio* lattice QCD because they are defined in terms of light-cone matrix elements that are not directly accessible on Euclidean lattices. Hence, PDFs are usually extracted from global analyses of different experiments [7–15].

Naturally a direct nonperturbative computation of PDFs is desirable: with sufficient precision, such a calculation would further constrain global fits in regions that may be experimentally inaccessible.

Until recently, lattice calculations have focused on determining the Mellin moments of PDFs, which are related to matrix elements of twist-2 operators that *can* be determined on the lattice [16–18]. The lattice regulator breaks Lorentz symmetry, which induces radiative mixing between operators of different mass dimensions. The resulting power divergences in the lattice spacing completely obscure the continuum limit. Moments up to the fourth moment can be extracted by carefully choosing the external momenta and operators, but this significantly limits the precision with which one can extract meaningful results for PDFs [19,20]. Beyond the fourth moment, power divergent mixing is inevitable, and this method cannot provide reliable calculations.

Ji recently proposed a new approach to directly extract PDFs from lattice calculations [21,22], based on a large-momentum effective theory [23]. Preliminary results first appeared in Ref. [24], but a number of issues remain, including a complete understanding of the renormalization of the relevant lattice matrix elements and the practical ability to resolve sufficiently large momenta on the lattice.

---

\*Department of Physics and Astronomy, University of Utah, Salt Lake City, Utah 84112, USA.

Here we propose a new formalism that removes mixing in the continuum limit and, in principle, enables the extraction of higher moments of PDFs from lattice QCD. We call this formalism the “smeared operator product expansion” (sOPE). We expand continuum matrix elements in a basis of locally smeared lattice degrees of freedom. The resulting matrix elements are functions of two scales, the smearing scale and the renormalization scale. The sOPE provides the framework necessary to relate these matrix elements, via Wilson coefficients, to phenomenologically useful quantities, such as the hadronic tensor of DIS.

Smearing has been widely used in lattice QCD to reduce ultraviolet fluctuations, partially restore rotational symmetry and thereby systematically improve the precision of lattice calculations [25–28]. For a pedagogical overview of smearing in lattice calculations, see, for example, Ref. [29]. In the sOPE, we implement smearing via the gradient flow, a classical evolution of the fields in a new dimension, the flow time, toward the stationary points of the action [30–34]. Matrix elements determined nonperturbatively on the lattice require no further renormalization, up to a fermionic wave function renormalization [30], and remain finite, provided the smearing scale is kept fixed in physical units in the continuum limit [31,35]. There are two further advantages: the gradient flow allows one to use smearing lengths of only one or two lattice spacings, much smaller than hadronic length scales on typical lattices, and therefore does not distort the low energy physics [36], and also the gradient flow is computationally very cheap.

The gradient flow is now well established as a tool to study lattice gauge theories, with applications from scale setting, i.e. determining the lattice spacing in physical units [37–41], to studying renormalization in lattice gauge theories. For example, the gradient flow has been used to define finite-volume renormalization schemes for the strong coupling constant [42–46], for operator renormalization [47], and to understand the nonperturbative scale dependence of renormalized matrix elements [48]. Related work has used Ward identities to study chiral fermions on the lattice [49] and the energy-momentum tensor [50–52].

In this paper we introduce the gradient flow for a single real scalar field with quartic interactions and outline some of the properties of the sOPE applied to real scalar field theory. Scalar field theories describe some important critical phenomena in nature, such as the antiferromagnetic phase transition, and have a long history as a testing ground for fundamental ideas in quantum field theory in four dimensions. For our purposes, the chief advantage is the simplicity of Euclidean scalar field theory, which lays bare the structure of the sOPE and highlights the points of similarity and contrast with the local operator product expansion (OPE).

In the next section, we review Wilson’s OPE and introduce the sOPE. We then apply the sOPE to scalar

field theory in Sec. III, illustrate how the gradient flow removes power-divergent mixing in Sec. IV, and calculate the perturbative Wilson coefficients to two loops in Sec. V. Finally, in Sec. VI, we study the scale dependence of the sOPE through renormalization group equations for the Wilson coefficients.

## II. OPERATOR PRODUCT EXPANSION

Wilson’s approach to the OPE for a nonlocal operator is widely known—see, for example, Ref. [53]—and here we review some notation necessary for our discussion.

We write the OPE for a nonlocal operator,  $\mathcal{Q}(x)$ , as

$$\mathcal{Q}(x) \stackrel{x \rightarrow 0}{\sim} \sum_k c_k(x, \mu) [\mathcal{O}^{(k)}(0)]_{\text{R}}. \quad (1)$$

The Wilson coefficients  $c_k(x, \mu)$  are complex functions of the spacetime separation,  $x$ , and renormalization scale,  $\mu$ , that capture the short-distance physics associated with the renormalized local operator  $[\mathcal{O}^{(k)}(0)]_{\text{R}}$ . We represent renormalized operators by  $[\dots]_{\text{R}}$  and suppress their dependence on the renormalization scale,  $\mu$ , for notational simplicity. The free-field mass dimension of the local operator determines the leading spacetime dependence of the corresponding Wilson coefficient.

As an example, let us consider the time-ordered two-point function of two scalar fields with spacetime separation  $x$ :  $\mathcal{T}\{\phi(x)\phi(0)\}$ . In free scalar field theory, the OPE is a Laurent expansion. Interactions generate subleading dependence on the spacetime separation in the Wilson coefficients, which become functions of the spacetime separation, the (renormalized) mass  $m_{\text{R}}$ , and the renormalization scale,  $\mu$ :

$$\mathcal{T}\{\phi(x)\phi(0)\} = \frac{c_{\parallel}(\mu x, m_{\text{R}}x)}{4\pi^2 x^2} \mathbb{1} + c_{\phi^2}(\mu x, m_{\text{R}}x) [\phi^2(0)]_{\text{R}} + \mathcal{O}(x). \quad (2)$$

Here we have factored out the leading spacetime dependence from the Wilson coefficients. The  $\mathcal{O}(x)$  indicates terms of order  $x$ , up to logarithmic corrections generated by interactions.

We propose replacing the set of local operators in the OPE by their locally smeared counterparts

$$\mathcal{Q}(x) \stackrel{x \rightarrow 0}{\sim} \sum_k d_k(\tau, x, \mu) \mathcal{S}^{(k)}(\tau, 0). \quad (3)$$

The Wilson coefficients,  $d_k(\tau, x, \mu)$ , and the smeared operators,  $\mathcal{S}^{(k)}(\tau, 0)$ , are now functions of an extra scale, the flow time,  $\tau$ . Nevertheless, the leading spacetime dependence of the Wilson coefficients is dictated by the canonical mass dimension of the corresponding smeared operator and is therefore just that of the standard OPE.

Just as the OPE is only valid for small spacetime separations, the sOPE requires small flow times. We will see that we require that  $\tau \propto x^2$ , where  $x$  is assumed to be small, to ensure that the Wilson coefficients are independent of the external states.

For example, returning to the time-ordered two-point function, the sOPE is

$$\begin{aligned} \mathcal{T}\{\phi(x)\phi(0)\} &= \frac{d_0(\mu x, \mu^2 \tau, m_R x)}{4\pi^2 x^2} \parallel \\ &+ d_{\rho^2}(\mu x, \mu^2 \tau, m_R x) \rho^2(\tau, 0) + \mathcal{O}(x, \tau), \end{aligned} \quad (4)$$

where we denote smeared fields at flow time  $\tau$  by  $\rho(\tau, x)$ .

In the following sections, we will observe four features of the smeared Wilson coefficients in the sOPE:

- (1) The logarithmic spacetime dependence of the original OPE is preserved in the sOPE.
- (2) The flow time serves as an ultraviolet regulator for the smeared Wilson coefficients, to leading order in perturbation theory.
- (3) Beyond leading order the flow time cannot regularize the Wilson coefficients because the flow evolution is classical. We can, however, absorb renormalization scale dependence into the renormalization parameters of the original theory.
- (4) For any OPE to be meaningful, the Wilson coefficients must be independent of the external states. We can ensure this for the sOPE by choosing  $s_{\text{rms}} < x$ ; i.e., the mean smearing radius must be smaller than the spacetime extent of the nonlocal operator. This ensures that the sOPE remains an expansion in approximately local operators. In other words, if the gradient flow probes length scales on the order of the nonlocal operator, then the sOPE becomes a poor expansion for the original operator.

Although we refer to this expansion as the *smeared* OPE, we really have in mind that the smearing is implemented via the gradient flow. The gradient flow acts as a smoothing operation that drives the degrees of freedom of the theory to the stationary points of the action. In QCD, the gradient flow corresponds to a continuous stout-smearing procedure, an analytic method for constructing lattice gauge fields with damped ultraviolet fluctuations [25]. The direct comparison of the gradient flow to other smearing schemes was first undertaken in Ref. [54].

Many studies of the gradient flow have incorporated a small flow-time expansion of fields at nonvanishing flow time in terms of local fields at zero flow time [48–52,55]. We can view such an expansion as an OPE in the flow time and thereby relate renormalized quantities calculated at nonzero flow time to the corresponding quantities in the original theory at vanishing flow time, which would otherwise be difficult to compute.

In this work, we take a different approach. We do not expand the flowed fields in terms of original fields at nonzero flow time but rather take as the fundamental objects of study the (matrix elements of) fields at positive flow time. Both approaches reflect the physically motivated expectation that smearing scales much smaller than the physical scales of the system should not distort the physics in question. The small flow-time expansion quantifies any deviations from this expectation and, furthermore, decouples analytic calculations of Wilson coefficients in the continuum from lattice calculations with smeared degrees of freedom. The sOPE incorporates the smearing scale as an inherent scale of the system, which requires new Wilson coefficients to be determined. Thus, both the small flow-time expansion and the sOPE are shaped by the role of the smearing scale as ultraviolet regulator and are related, but distinct, conceptual approaches to the same physics: partially restoring rotational symmetry on the lattice.

Smearing, in general, is a tool that partially restores rotational symmetry [36] and thereby improves the continuum limit of lattice calculations. Smearing via the gradient flow has a number of advantages. In particular, matrix elements determined nonperturbatively on the lattice using smeared degrees of freedom require no further renormalization [32], up to fermionic wave function renormalization [30], and remain finite, provided the smearing scale is kept fixed in physical units as the continuum limit is taken.

We now turn to a more complete study of the sOPE applied to  $\phi^4$  scalar field theory, a particularly straightforward theory in which to examine the sOPE. We can solve the flow-time equations exactly because the flow-time evolution is linear in the scalar field. We do not need to consider the complications associated with gauge fixing [31,32] nor the extra renormalization of fermions [30]. Furthermore, for scalar fields the sOPE can be understood to be simply a resummation of the original OPE. Although it is not necessary for our work, it is also interesting to note that the OPE is known to converge for Euclidean  $\phi^4$  theory in four dimensions, at a fixed but arbitrary order in the perturbative expansion [56]. This result holds at arbitrary spacetime separations, provided the external states are of compact support.

Looking toward future calculations in QCD, we anticipate that the technical issues associated with a flow equation that incorporates gauge field interactions will slightly complicate the perturbative calculations by increasing the number of diagrams at a given order in perturbation theory but will not alter our conclusions. Within the gauge sector, there are no loops of flowed fields because renormalized correlation functions remain finite at nonzero flow time [31]. Therefore, at leading order in perturbation theory, the flow time regulates ultraviolet divergences; beyond leading order an appropriate renormalization procedure must be incorporated. With fermionic fields there is

an extra fermion renormalization parameter, calculated in Ref. [30], but this can be removed by considering renormalization group invariant quantities [30]. We also note that all perturbative calculations for the sOPE can be carried out in the continuum and do not require lattice perturbation theory, which is generally more involved [57,58].

### III. GRADIENT FLOW FOR SCALAR FIELD THEORY

We work in four-dimensional Euclidean scalar field theory with quartic self-interactions and bare mass  $m$ , defined by the action

$$S_\phi[\phi] = \frac{1}{2} \int d^4x \left[ (\partial_\nu \phi)^2 + m^2 \phi^2 + \frac{\lambda}{12} \phi^4 \right]. \quad (5)$$

To study the sOPE, we introduce the scalar gradient flow, which we define through the flow-time evolution equation

$$\frac{\partial \rho(\tau, x)}{\partial \tau} = \partial^2 \rho, \quad (6)$$

where  $\rho$  is a scalar field at nonzero flow time,  $\tau$ , and  $\partial^2$  is the Euclidean, four-dimensional Laplacian operator. Note that the flow time has units  $[\tau] = [x]^2$ .

Imposing the Dirichlet boundary condition  $\rho(0, x) = \phi(x)$ , we may write the exact solution of the flow-time equation as

$$\rho(\tau, x) = e^{\tau \partial^2} \phi(x) \quad (7)$$

or, in the momentum representation, as

$$\tilde{\rho}(\tau, p) = e^{-\tau p^2} \tilde{\phi}(p). \quad (8)$$

The full solution is

$$\begin{aligned} \rho(\tau, x) &= \int d^4y \int \frac{d^4p}{(2\pi)^4} e^{ip \cdot (x-y)} e^{-\tau p^2} \phi(y) \\ &= \frac{1}{16\pi^2 \tau^2} \int d^4y e^{-(x-y)^2/4\tau} \phi(y), \end{aligned} \quad (9)$$

which demonstrates explicitly the ‘‘smearing’’ effect of the gradient flow: the flow time exponentially suppresses ultraviolet modes. We parametrize the smearing radius via the root-mean-square smearing length,  $s_{\text{rms}} = \sqrt{8\tau}$ .

The (Euclidean) smeared scalar propagator, for two fields at flow times  $\tau_1$  and  $\tau_2$ , is given by

$$\tilde{G}_\rho(\tau_1, \tau_2, k) = \frac{e^{-(\tau_1 + \tau_2)k^2}}{k^2 + m^2}. \quad (10)$$

The flow-time evolution is classical, so any interactions must occur at zero flow time. The corresponding Feynman

rule for the four-point vertex is just that of the standard (Euclidean) four-point vertex,  $V^{(4)} = -\lambda/24$ .

### IV. MIXING ON THE LATTICE

Before we examine the sOPE in detail, we demonstrate how the gradient flow removes power-divergent mixing on the lattice. We consider the example of twist-2 operators in scalar field theory, which are symmetric and traceless and given by

$$T_{\mu_1 \dots \mu_n}(x) = \phi(x) \partial_{\mu_1} \dots \partial_{\mu_n} \phi(x) - \text{traces}. \quad (11)$$

On the lattice, we replace the partial derivatives with discrete difference operators

$$T_{\mu_1 \dots \mu_n}^{\text{latt}}(x) = \phi(x) \Delta_{\mu_1} \dots \Delta_{\mu_n} \phi(x) - \text{traces}. \quad (12)$$

The spacetime point  $x$  is now a node in the lattice,  $x_\mu = a n_\mu$ , where  $a$  is the lattice spacing and  $n_\mu$  is a four-component lattice vector. The discrete difference operators can be improved to remove discretization effects, but the simplest such symmetric operator acts on a scalar field as

$$\Delta_\mu \phi(x) = \frac{1}{2a} (\phi(x + \hat{\mu}) - \phi(x - \hat{\mu})), \quad (13)$$

where  $\hat{\mu}$  is the unit vector in the  $\mu$ th direction.

The lattice regulator breaks rotational symmetry, which induces mixing between twist-2 operators of different mass dimension. On dimensional grounds, the mixing coefficients scale with inverse powers of the lattice spacing, and these coefficients diverge in the continuum limit. This is the problem of power-divergent mixing on the lattice. For example, the simple bilinear  $T^{\text{latt}}(x) = \phi(x)\phi(x)$  mixes with the operator  $T_{\mu\nu}^{\text{latt}}(x)$  with a coefficient that scales as  $1/a^2$ . More generally, the mixing between  $T^{\text{latt}}(x)$  and any twist-2 operator with an even number of derivatives,  $T_{\mu_1 \dots \mu_{2n}}^{\text{latt}}(x)$ , scales as  $1/a^{2n}$ .

The smeared counterparts of these operators, which are given by

$$S_{\mu_1 \dots \mu_n}^{\text{latt}}(x) = \rho(\tau, x) \Delta_{\mu_1} \dots \Delta_{\mu_n} \rho(\tau, x) - \text{traces}, \quad (14)$$

do not suffer from this problem. The mixing coefficient between  $S^{\text{latt}}(x) = \rho(\tau, x)\rho(\tau, x)$  and  $S_{\mu_1 \dots \mu_{2n}}^{\text{latt}}(x)$  scales as  $1/\tau^n$ , where  $\tau$  is the flow time in *physical units*. Provided we keep the dimensionful scale  $\tau = \tilde{\tau} a^2$  fixed, where  $\tilde{\tau}$  is dimensionless, then as the lattice spacing  $a$  decreases, the mixing coefficient remains finite, because matrix elements at nonzero flow time cannot contain any additional divergences [31,35].

As a simple illustration of this behavior, let us consider the matrix element of two twist-2 operators of different mass dimension:

$$M_{\text{cont}} = \langle \Omega | \phi(0) \phi(0) \phi(0) \partial_\mu \partial_\nu \phi(0) | \Omega \rangle. \quad (15)$$

This matrix element vanishes for massless scalar fields. On the lattice, however, the corresponding matrix element,

$$M_{\text{latt}} = \langle \Omega | \phi(0) \phi(0) \phi(0) \Delta_\mu \Delta_\nu \phi(0) | \Omega \rangle, \quad (16)$$

is nonzero.

We show the Feynman diagram for the leading contribution to this matrix element in the left-hand diagram of Fig. 1, which is given by

$$M_{\text{latt}}^{(0)} = \frac{1}{a^4} \int_{-\pi/a}^{\pi/a} \frac{d^4(ak)}{(2\pi)^4} \frac{\hat{k}_\mu \hat{k}_\nu}{(\hat{k}^2 + m_0^2)^2}, \quad (17)$$

where  $\hat{k}_\mu = (2/a) \sin(ak_\mu/2)$ . We have included a bare mass  $m_0$  to remove spurious infrared divergences, but the integral is finite, and we can take the massless limit,  $m_0 \rightarrow 0$ , to match to the continuum massless theory. We expand this in powers of the lattice spacing to obtain

$$\begin{aligned} M_{\text{latt}}^{(0)} &= -\frac{\delta_{\mu\nu}}{4} \int_{-\pi/a}^{\pi/a} \frac{d^4k}{(2\pi)^4} \frac{k^2}{(k^2 + m_0^2)^2} + \mathcal{O}(a^2) \\ &= -\frac{\delta_{\mu\nu}}{48a^2} + \mathcal{O}(a^0) \end{aligned} \quad (18)$$

in the massless limit. This result signals the appearance of power-divergent mixing: the  $1/a^2$  term diverges in the continuum limit. Although this calculation is only leading order in perturbation theory, higher-order contributions do not modify this power-divergent dependence on the lattice spacing [36].

If we calculate this matrix element with smeared degrees of freedom (which we depict in the right-hand diagram of Fig. 1), however, we find

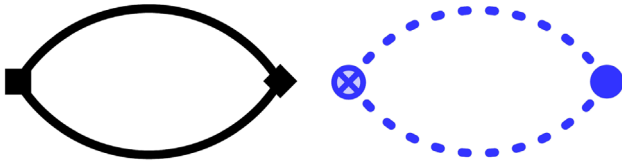


FIG. 1 (color online). Diagrams representing the leading contributions to the mixing matrix elements with unsmearred fields,  $M_{\text{latt}}^{(0)}$  and smeared fields,  $M_{\text{latt}}^{(0)}(\tau)$ . The black solid lines in the left-hand diagram represent unsmearred propagators, and the black solid square and diamond are the operators  $\phi^2(0)$  and  $\phi(0) \Delta_\mu \Delta_\nu \phi(0)$ . The blue dashed lines in the right-hand diagram are smeared propagators, and the two different blue blobs, filled and unfilled, represent the smeared operators  $\rho^2(\tau, 0)$  and  $\rho(\tau, 0) \Delta_\mu \Delta_\nu \rho(\tau, 0)$ .

$$\begin{aligned} M_{\text{latt}}^{(0)}(\tau) &= \langle \Omega | \rho(\tau, 0) \rho(\tau, 0) \rho(\tau, 0) \Delta_\mu \Delta_\nu \rho(\tau, 0) | \Omega \rangle \\ &= -\frac{\delta_{\mu\nu}}{4} \int_{-\pi/a}^{\pi/a} \frac{d^4k}{(2\pi)^4} \frac{k^2 e^{-4\tau k^2}}{(k^2 + m_0^2)^2} + \mathcal{O}(a^2) \\ &= \delta_{\mu\nu} \frac{e^{-4\pi^2\tau/a^2} - 1}{256\pi^2\tau} + \mathcal{O}(a^0). \end{aligned} \quad (19)$$

Once again we have taken the massless limit. In the continuum limit, keeping the flow time  $\tau$  fixed in physical units, this matrix element tends to a constant, signaling the suppression of power-divergent mixing for smeared degrees of freedom.

## V. WILSON COEFFICIENTS FOR THE SOPE

The procedure for calculating smeared Wilson coefficients parallels that for the OPE, discussed in, for example, Ref. [53]. With the Feynman rules of Sec. III in hand, the calculation of smeared Wilson coefficients up to next-to-leading order in perturbation theory is straightforward. We determine the smeared Wilson coefficients for the leading connected and disconnected operators, starting with the disconnected contribution.

### A. Disconnected contributions

#### 1. Leading order

We illustrate the leading-order (tree-level) and next-to-leading-order (one-loop) contributions to the smeared Wilson coefficient for the disconnected operator,  $\mathbb{1}$ , in Fig. 2. As we will see, the leading-order contribution is independent of the renormalization scale,  $\mu$ , because at this order the flow time serves as the ultraviolet regulator. Beyond leading order, however, the smeared Wilson coefficient will have a renormalization scale dependence.

We extract the disconnected smeared Wilson coefficient by considering matrix elements of each of the operators in the sOPE in the vacuum, which removes any connected contributions. To  $\mathcal{O}(x)$  we have

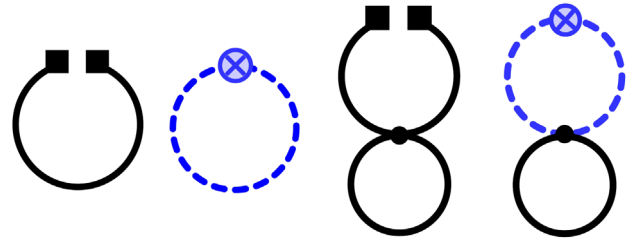


FIG. 2 (color online). Diagrams representing the contributions to the Wilson coefficient  $d_1$  at leading order (left two diagrams) and next-to-leading order (right two diagrams). Solid black and dashed blue lines are propagators at vanishing and nonvanishing flow times, respectively. The black squares are unsmearred fields  $\phi(0)$ , black dots are interaction vertices at vanishing flow time, and the blue blob represents the smeared operator  $\rho^2(\tau, 0)$ .

$$\begin{aligned} & \langle \Omega | \mathcal{T} \{ \phi(x) \phi(0) \} | \Omega \rangle \\ &= \frac{d_{\parallel}(\mu x, \mu^2 \tau, mx)}{4\pi^2 x^2} \langle \Omega | \parallel | \Omega \rangle \\ &+ d_{\rho^2}(\mu x, \mu^2 \tau, mx) \langle \Omega | \rho^2(\tau, 0) | \Omega \rangle + \mathcal{O}(x), \end{aligned} \quad (20)$$

Here we have chosen the normalization of  $d_{\parallel}$  so that at leading order in the free theory  $d_{\parallel}$  is unity. We expand each quantity in this expression to one loop according to

$$f = f^{(0)} - \lambda f^{(1)} + \mathcal{O}(\lambda^2), \quad (21)$$

where  $f$  stands for either a matrix element or Wilson coefficient. We have chosen the sign of the one-loop contribution to factor out the sign of the coupling constant arising from the Feynman rule for the four-point vertex  $V^{(4)} = -\lambda/24$ .

The tree-level Wilson coefficient is then given by the small spacetime behavior of

$$\begin{aligned} \frac{d_{\parallel}^{(0)}}{4\pi^2 x^2} \stackrel{x \rightarrow 0}{=} & \{ \langle \Omega | \mathcal{T} \{ \phi(x) \phi(0) \} | \Omega \rangle \\ & - \langle \Omega | \rho^2(\tau, 0) | \Omega \rangle \}_{\mathcal{O}(m^2)}, \end{aligned} \quad (22)$$

where we have neglected the arguments of the coefficient for clarity and used the fact that the tree-level connected coefficient is  $d_{\rho^2}^{(0)} = 1$ . The subscript indicates that we must expand the result to  $\mathcal{O}(m^2)$ . For more details about the calculation of Wilson coefficients see, for example, Ref. [53]. The corresponding Feynman integral representation is

$$\begin{aligned} d_{\parallel}^{(0) x \rightarrow 0} &= 4\pi^2 x^2 \left\{ \int_k \frac{e^{ik \cdot x} - e^{-2k^2 \tau}}{k^2 + m^2} \right\}_{\mathcal{O}(m^2)} \\ &= 4\pi^2 x^2 \int_k (e^{ik \cdot x} - e^{-2k^2 \tau}) \left( \frac{1}{k^2} - \frac{m^2}{(k^2)^2} \right), \end{aligned} \quad (23)$$

where

$$\int_k \equiv \int \frac{d^4 k}{(2\pi)^4}. \quad (24)$$

The smeared Wilson coefficient is

$$d_{\parallel}^{(0)} = 1 - \frac{x^2}{8\tau} + \frac{m^2 x^2}{4} \left[ \gamma_E - 1 + \log \left( \frac{x^2}{8\tau} \right) \right], \quad (25)$$

with  $\gamma_E \approx 0.577216$  the Euler–Mascheroni constant.

We can compare this result with the Wilson coefficient for the OPE for  $d = 4 - 2\epsilon$  dimensions [53]:

$$\bar{c}_{\parallel}^{(0)} = 1 + \frac{m^2 x^2}{4} \left[ \frac{1}{\epsilon} + 1 + \gamma_E + \log \left( \frac{\pi \mu^2 x^2}{4} \right) \right]. \quad (26)$$

Then in the  $\overline{MS}$  scheme, this becomes

$$\bar{c}_{\parallel}^{(0)} = 1 + \frac{m^2 x^2}{4} \left[ 1 + 2\gamma_E + \log \left( \frac{\mu^2 x^2}{16} \right) \right]. \quad (27)$$

Although the finite contribution to these expressions cannot be directly compared, because we have expressed the Wilson coefficients in two different renormalization schemes, we note three important features. First, the logarithmic dependence on the spacetime separation is identical. Second, the flow time  $\tau$  plays the role of the renormalization scale at leading order. Third, we see that for small spacetime separations we require a small flow-time parameter. If we do not choose the flow-time parameter appropriately, we generate large logarithmic contributions to the smeared Wilson coefficients, and the sOPE exhibits poor convergence properties, even at small spacetime separations.

## 2. Next-to-leading order

At one loop, the smeared Wilson coefficient is given by

$$\begin{aligned} -\lambda \frac{d_{\parallel}^{(1)}}{4\pi^2 x^2} &= \{ \langle \Omega | \mathcal{T} \{ \phi(x) \phi(0) \} | \Omega \rangle \\ &- \langle \Omega | \rho^2(\tau, 0) | \Omega \rangle \}_{\mathcal{O}(m^2)}^{(1)}. \end{aligned} \quad (28)$$

The four-point interaction in this diagram, which we show in Fig. 2, appears at zero flow time. Therefore, the flow time cannot act as a regulator for the momentum integral over  $k_2$ , and we must introduce a renormalization procedure. We use dimensional regularization and the  $\overline{MS}$  scheme. The double integral is straightforward, however, because the two integrals can be carried out separately:

$$\frac{d_{\parallel}^{(1)}}{4\pi^2 x^2} = \left\{ \int_{k_1} \frac{e^{ik_1 \cdot x} - e^{-2k_1^2 \tau}}{(k_1^2 + m^2)^2} \frac{1}{2} \int_{k_2} \frac{1}{k_2^2 + m^2} \right\}_{\mathcal{O}(m^2)}. \quad (29)$$

We find, for  $m > 0$ ,

$$d_{\parallel}^{(1)} = -\frac{m^2 x^2}{128\pi^2} \left[ \gamma_E - 1 + \log \left( \frac{x^2}{8\tau} \right) \right] \left[ 1 + \log \left( \frac{\mu^2}{m^2} \right) \right]. \quad (30)$$

Here we see that the second term, which is a function of the new renormalization scale,  $\mu$ , and the bare mass,  $m$ , is nothing other than the one-loop contribution to the mass renormalization of the original theory, in the  $\overline{MS}$  scheme [59]. Moreover, the factor containing the flow time is identical to the  $\mathcal{O}(m^2)$  term from the leading-order contribution,  $d_{\parallel}^{(0)}$ , in Eq. (25).

Therefore, we can simply combine the leading-order and next-to-leading-order terms to give

$$d_0 = 1 - \frac{x^2}{8\tau} + \frac{m_R^2 x^2}{4} \left[ \gamma_E - 1 + \log\left(\frac{x^2}{8\tau}\right) \right] + \mathcal{O}(\lambda^2), \quad (31)$$

where  $m_R$  is the renormalized mass in the  $\overline{MS}$  scheme, given by  $m_R^2 = Z_m^{-1} m^2$  and  $Z_m$  is the mass renormalization [59]:

$$Z_m = 1 + \frac{\lambda}{16\pi^2} \left[ 1 + \log\left(\frac{\mu^2}{m^2}\right) \right] + \mathcal{O}(\lambda^2). \quad (32)$$

This is a clear, next-to-leading-order example of how the divergences of the theory at nonzero flow time are absorbed by the renormalization parameters of the original theory at zero flow time. In other words, the renormalized theory at zero flow time remains ultraviolet finite at nonzero flow time.

## B. Connected contribution

We illustrate the leading- and next-to-leading-order contributions to the connected Wilson coefficient  $d_{\rho^2}(\mu x, \mu^2 \tau, \mu x)$  of Eq. (4) in Figs. 3 and 4, respectively. Throughout this section, we neglect diagrams that are trivially incorporated as part of the wave function renormalization of the external fields, such as the one-loop examples illustrated in Fig. 5. Provided the original theory at zero flow time is renormalized, counterterms cancel these contributions completely.

### 1. Leading order

We extract the leading-order connected Wilson coefficient by considering matrix elements of each of the operators in the sOPE coupled to two external fields, which removes any disconnected contributions. We can then read off the one-loop contribution to the Wilson coefficient,  $d_{\rho^2}^{(1)}$ , by matching terms at  $\mathcal{O}(\lambda)$ . This contribution is given by the small spacetime behavior of

$$-\lambda d_{\rho^2}^{(1)x \rightarrow 0} \{ \langle \Omega | \mathcal{T} \{ \phi(x) \phi(0) \} \tilde{\phi}(p_1) \tilde{\phi}(p_2) | \Omega \rangle^{(1)} - \langle \Omega | \rho^2(\tau, 0) \tilde{\phi}(p_1) \tilde{\phi}(p_2) | \Omega \rangle^{(1)} \}_{\mathcal{O}(m^0)}. \quad (33)$$

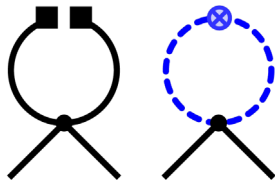


FIG. 3 (color online). Diagrams representing the leading-order (one-loop) contributions to the Wilson coefficient  $d_{\rho^2}$ . Details of the Feynman diagrams are provided in the caption of Fig. 2.

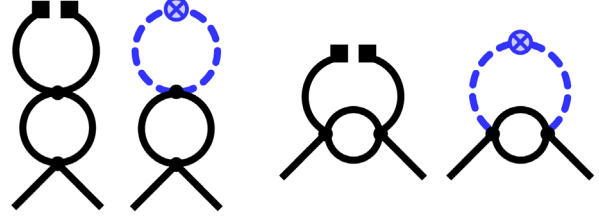


FIG. 4 (color online). Diagrams representing the contributions to the next-to-leading-order (two-loop) contributions to the Wilson coefficients  $d_{\rho^2}$ . For details of the Feynman diagrams, see the caption of Fig. 2.

The corresponding Feynman integral is

$$\frac{1}{(p_1^2 + m^2)(p_2^2 + m^2)} \left\{ \frac{1}{2} \int_k \frac{e^{ik \cdot x} - e^{-(k^2 + q^2)\tau}}{(k^2 + m^2)(q^2 + m^2)} \right\}, \quad (34)$$

where  $q = k - p_1 - p_2$ . We extract the smeared Wilson coefficient by examining the small spacetime behavior of the integral in curly braces, expanded to  $\mathcal{O}(m^0)$ :

$$d_{\rho^2}^{(1)x \rightarrow 0} \left\{ \frac{1}{2} \int_k \frac{e^{ik \cdot x} - e^{-(k^2 + q^2)\tau}}{(k^2 + m^2)(q^2 + m^2)} \right\}_{\mathcal{O}(m^0)}. \quad (35)$$

The smeared Wilson coefficients must be independent of the external states to ensure that the sOPE is truly an operator expansion. In this particular case, we require that  $d_{\rho^2}^{(1)}$  is independent of the external momenta  $p_1$  and  $p_2$  and the mass. By taking a derivative with respect to one of the external momenta,

$$\frac{d}{dp_i} d_{\rho^2}^{(1)} = \int_k \frac{q_i [e^{ik \cdot x} - e^{-(k^2 + q^2)\tau} (1 + (q^2 + m^2)\tau)]}{(k^2 + m^2)(q^2 + m^2)^2}, \quad (36)$$

we obtain a convergent integral. The  $x \rightarrow 0$  limit of this integral is now well defined and only vanishes if the flow time is related to the spacetime separation. An analogous result holds if we take a derivative with respect to the external mass,  $m$ . On dimensional grounds, then, we

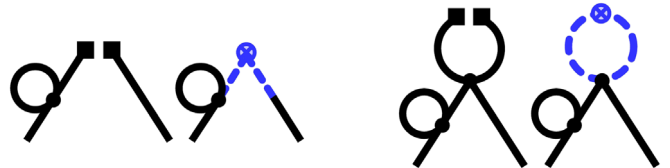


FIG. 5 (color online). Example diagrams that are naturally incorporated in the renormalized external propagators. We do not include these contributions in our explicit calculations of the Wilson coefficients. For details of the Feynman diagrams, see the caption of Fig. 2.



guarantee that the smeared Wilson coefficient is independent of the external states by choosing  $\tau \propto x^2$ .

On physical grounds, however, we require that the smearing radius is smaller than the spacetime extent of the nonlocal operator:  $s_{\text{rms}} < x$ . This choice ensures that the sOPE remains an expansion in local operators. Physically speaking, if the gradient flow probes length scales on the order of the nonlocal operator, which we represent in Fig. 6, then smeared operators would cease to be (approximately) local. In other words, the sOPE would be a poor expansion for the original operator. This is the physical origin of the third feature that we saw in the leading-order disconnected contribution, Eq. (25): small spacetime separations require small flow times to ensure convergence. The OPE requires small spacetime separations for good convergence, so it follows that the sOPE requires small flow times as well.

There is a complementary viewpoint that elucidates the small flow-time requirement more quantitatively: the small flow-time expansion [31,50,52]. In this case we see that the derivative of Eq. (36) is independent of the external momenta in the  $x \rightarrow 0$  limit, up to terms linear in the flow time:

$$\frac{d}{dp_i} d_{\rho^2}^{(1)} = \int_k \frac{q_i(e^{ik \cdot x} - 1)}{(k^2 + m^2)(q^2 + m^2)^2} + \mathcal{O}(\tau). \quad (37)$$

From this, it is clear that the Wilson coefficients will be independent of the external states, up to terms linear in the flow time. Therefore, provided the flow time is small relative to the spacetime separation, the sOPE is an expansion in approximately local operators, in a quantifiable sense. Moreover, the flow-time dependence will cancel in the product of the Wilson coefficient and its associated matrix element, to the desired order in the flow time.

We are free to set  $p_1 = p_2 = 0$  in Eq. (35) because the smeared Wilson coefficient is independent of the external momenta and the mass to the order at which we are working [53]. Expanding in the mass, we obtain

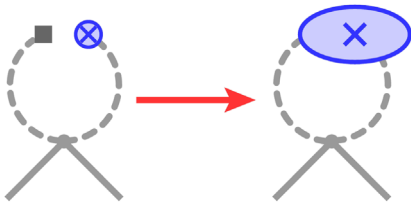


FIG. 6 (color online). At small flow times (left-hand diagram), the smeared operators are localized relative to the spacetime separation of the nonlocal operator. At large flow-time values (right-hand diagram), however, the smearing radius probes the scale of the nonlocal, and the sOPE is a poor approximation to the original nonlocal operator. For details of the Feynman diagrams, see the caption of Fig. 2.

$$\begin{aligned} d_{\rho^2}^{(1)} &= \frac{1}{2} \int_k \frac{e^{ik \cdot x} - e^{-2k^2 \tau}}{(k^2)^2} \\ &= -\frac{1}{32\pi^2} \left[ \gamma_E - 1 + \log\left(\frac{x^2}{8\tau}\right) \right]. \end{aligned} \quad (38)$$

Combining this with the leading-order contribution, which is just unity, we have

$$d_{\rho^2} = 1 + \frac{\lambda}{32\pi^2} \left[ \gamma_E - 1 + \log\left(\frac{x^2}{8\tau}\right) \right] + \mathcal{O}(\lambda^2). \quad (39)$$

In contrast, the Wilson coefficient for the OPE in the  $\overline{MS}$  scheme, denoted by  $\bar{c}$ , is

$$\bar{c}_{\phi^2} = 1 + \frac{\lambda}{32\pi^2} \left[ 1 + 2\gamma_E + \log\left(\frac{\mu^2 x^2}{16}\right) \right] + \mathcal{O}(\lambda^2). \quad (40)$$

We note the occurrence of the three features we observed for the leading-order disconnected contribution: the same spacetime dependence for both smeared and unsmeared coefficients, the appearance of the flow time as a leading-order regulator, and the need to choose a small flow time for small spacetime separations to avoid large logarithmic contributions. From the small flow-time expansion viewpoint, we can confirm that the flow-time dependence ultimately cancels to the desired order. For example, the matrix element of  $\rho^2(\tau, 0)$  coupled to two external fields is

$$\begin{aligned} &\langle \Omega | \rho^2(\tau, 0) \tilde{\phi}(p_1) \tilde{\phi}(p_2) | \Omega \rangle \\ &= 1 + \frac{\lambda}{32\pi^2} [1 + \gamma_E + \log(2m^2 \tau)] + \mathcal{O}(\tau, \lambda^2) \end{aligned} \quad (41)$$

for sufficiently small flow times. Here we have dropped the external fields, which we take to be on shell, for simplicity. The product of this matrix element with the Wilson coefficient is independent of the flow time to one loop and  $\mathcal{O}(\tau)$ , as we would expect:

$$\begin{aligned} &d_{\rho^2} \langle \Omega | \rho^2(\tau, 0) \tilde{\phi}(p_1) \tilde{\phi}(p_2) | \Omega \rangle \\ &= 1 + \frac{\lambda}{32\pi^2} \left[ 2\gamma_E + \log\left(\frac{m^2 x^2}{4}\right) \right] + \mathcal{O}(\tau, \lambda^2). \end{aligned} \quad (42)$$

## 2. Next-to-leading order

To determine the next-to-leading-order contribution to the connected Wilson coefficient, we must incorporate the Feynman diagrams of Fig. 4. The two-loop diagrams of Fig. 7 do not contribute to the Wilson coefficient  $d_{\rho^2}$  because they appear at  $\mathcal{O}(m^2)$ .

Looking at the Feynman diagrams of Fig. 4, and bearing in mind our experience of the next-to-leading-order contribution to  $d_{\mathbb{1}}$ , we immediately observe that these diagrams are simply the product of the one-loop Wilson coefficient,

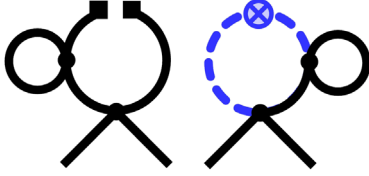


FIG. 7 (color online). Two-loop diagrams that appear at  $\mathcal{O}(m^2)$  and therefore do not contribute to  $d_{\rho^2}$ . For details of the Feynman diagrams, see the caption of Fig. 2.

$d_{\rho^2}^{(1)}$ , and the next-to-leading-order renormalized four-point vertex. This contribution to the vertex is, of course, nothing other than the next-to-leading-order contribution to the renormalized coupling constant. Thus, we write the Wilson coefficient quite simply as

$$d_{\rho^2} = 1 + \frac{\lambda_R}{32\pi^2} \left[ \gamma_E - 1 + \log\left(\frac{x^2}{8\tau}\right) \right] + \mathcal{O}(\lambda^3), \quad (43)$$

where  $\lambda_R$  is the renormalized coupling. In the  $\overline{MS}$  scheme, the renormalized coupling is given by

$$\lambda_R = \lambda - \frac{3\lambda^2}{2(16\pi^2)} \log\left(\frac{\mu^2}{m^2}\right) + \mathcal{O}(\lambda^3). \quad (44)$$

For a calculation of this to five loops, see Ref. [59].

As we move beyond the leading-order Wilson coefficients, i.e.,  $d_1^{(0)}$  and  $d_{\rho^2}^{(1)}$ , divergent radiative corrections appear in our calculations because all field interaction vertices appear at zero flow time. These divergences can be removed by the renormalization parameters of the original theory, and the renormalization scale dependence of the smeared operators is completely contained in the renormalization parameters of the original theory. This is to be expected: it follows from the fact that renormalized matrix elements at zero flow time remain finite at nonzero flow time and require no further renormalization [31,35].

Ultimately, for realistic calculations in lattice QCD, the perturbative calculation of smeared Wilson coefficients must be combined with nonperturbative determinations of matrix elements at hadronic energy scales. Scalar  $\phi^4$  theory is not asymptotically free in four dimensions, but we can understand the mathematical features of the sOPE in more detail by studying the renormalization group equations for the simple example of scalar fields.

## VI. RENORMALIZATION GROUP EQUATIONS

We consider the matrix elements of scalar operators coupled to  $N$  external, unsmeared scalar fields. We can derive renormalization group equations for the Wilson coefficients of the OPE by considering the scale dependence of suitably chosen Green functions [53]. The Green function for  $N + 2$  external scalar fields obeys the renormalization group equation

$$\left[ \mu \frac{d}{d\mu} + (N + 2)\gamma \right] \langle \Omega | \tilde{\phi}(p_1) \dots \tilde{\phi}(p_{N+2}) | \Omega \rangle = 0, \quad (45)$$

while the Green function of the renormalized operator  $\phi_R^2(0)$  coupled to  $N$  external scalar fields satisfies

$$\left[ \mu \frac{d}{d\mu} - \gamma_m + N\gamma \right] \langle \Omega | \phi_R^2(0) \tilde{\phi}(p_1) \dots \tilde{\phi}(p_N) | \Omega \rangle = 0. \quad (46)$$

Here the renormalization group operator for scalar field theory is

$$\mu \frac{d}{d\mu} = \mu \frac{\partial}{\partial \mu} \Big|_{\lambda, m_R} + \beta \frac{\partial}{\partial \lambda} \Big|_{\mu, m_R} - \gamma_m m_R \frac{\partial}{\partial m_R} \Big|_{\mu, \lambda}, \quad (47)$$

and the coefficients are [59]

$$\beta^{\overline{MS}}(\lambda) = \mu \frac{d\lambda}{d\mu} = \frac{3\lambda^2}{(16\pi^2)^2} + \mathcal{O}(\lambda^3), \quad (48)$$

$$\begin{aligned} \gamma_m^{\overline{MS}}(\lambda) &= -\frac{\mu}{2} \frac{d \log(m_R)}{d\mu} \\ &= -\frac{\lambda}{2(16\pi^2)} + \frac{5\lambda^2}{12(16\pi^2)^2} + \mathcal{O}(\lambda^3), \end{aligned} \quad (49)$$

$$\gamma^{\overline{MS}}(\lambda) = \frac{\mu}{2} \frac{d \log(Z_\phi)}{d\mu} = \frac{\lambda^2}{12(16\pi^2)^2} + \mathcal{O}(\lambda^3). \quad (50)$$

In general these coefficients depend on the mass, the renormalization scale, and the renormalized coupling constant, but in a mass independent renormalization scheme, such as the  $\overline{MS}$  scheme, they depend on the renormalization scale only through the renormalized coupling constant. These functions are known to five loops for the  $O(N)$ -symmetric theory, given by the  $N$ -multiplet  $\Phi = \{\phi_1, \dots, \phi_N\}$  [59,60].

Returning again to our example of the OPE for the two-point function, Eq. (2), we can derive a renormalization group equation for the Wilson coefficient  $c_{\phi^2}$  by coupling these operators to two external scalar fields and using Eqs. (45) and (46) (for further details, see, for example, Ref. [53]):

$$\left[ \mu \frac{d}{d\mu} + 2(\gamma + \gamma_m) \right] c_{\phi^2} = 0. \quad (51)$$

Just as we might expect, the anomalous dimension of the Wilson coefficient  $c_{\phi^2}$  is equal to the difference between the anomalous dimension of  $\phi(x)\phi(0)$  and that of  $[\phi^2(0)]_R$ .

### A. Renormalization group equations for the sOPE Wilson coefficients

The flow time,  $\tau$ , introduces a new scale into the problem. In principle one can view the flow time as just another external scale, unrelated to the renormalization scale  $\mu$ . In this case, it is natural to modify the renormalization group equations to account for the change in the Green functions as we change both  $\mu$  and  $\tau$ :

$$\mu \frac{d}{d\mu} \rightarrow \mu \frac{d}{d\mu} - 2\tau \frac{d}{d\tau}. \quad (52)$$

Our choice of differential operator is constrained by the mass dimension of each scale,  $\mu$  and  $\tau$ , but is not unique. In particular, one could choose the operator  $\mu d/d\mu + \tau d/d\tau$ . This freedom does not affect the logic of our discussion nor our conclusion because alternative conventions can be absorbed into the definition of the renormalization parameters and anomalous dimensions in, for example, Eq. (58).

At this stage it is worth commenting on the two scales in the problem,  $\mu$  and  $\tau$ . In DIS, the spacetime separation of the corresponding OPE,  $x$ , and renormalization scale,  $\mu$ , are, in principle, two distinct scales. The spacetime separation is provided by the inverse momentum transfer of a particular DIS experiment or set of experiments. The renormalization scale, however, is a theoretical choice, and ultimately physical quantities should not depend on the renormalization scale. It is generally convenient to choose  $\mu = 1/x$ , but it is not strictly necessary.

The relationship between the flow time and the renormalization scale is analogous, and these two scales are distinct. For the sOPE, the flow time can be considered as simply an external scale, imposed by some particular lattice ‘‘experiment,’’ and the renormalization scale is a convenient theoretical choice. We will see that it is helpful to tie these scales together, to reduce the two-scale problem to a single scale, but this is not formally necessary. Therefore, in the following analysis, the flow and renormalization scale should be understood as completely independent scales.

Considering again the sOPE for the two-point function, Eq. (4), we determine the renormalization group equation for the smeared Wilson coefficient,  $d_{\rho^2}$ , by following a procedure analogous to that outlined above.

We assume that we are working in the small flow-time regime, which allows us to relate operators at vanishing and nonvanishing flow time [31,50,52]:

$$[\phi^2(0)]_R = \mathcal{Z}_{\rho^2}(\tau, \mu) \rho^2(\tau, 0) + \mathcal{O}(\tau). \quad (53)$$

This coefficient satisfies

$$\mu \frac{d}{d\mu} \log(\mathcal{Z}_{\rho^2}(\tau, \mu^2)) = 2\gamma_m \quad (54)$$

and to one loop is given by

$$\mathcal{Z}_{\rho^2}(\tau, \mu^2) = 1 - \frac{\lambda}{32\pi^2} [1 + \gamma_E + \log(2\tau\mu^2)] + \mathcal{O}(\lambda^2, \tau). \quad (55)$$

We apply the renormalization group operator

$$\mu \frac{d}{d\mu} - 2\tau \frac{d}{d\tau} + (N+2)\gamma \quad (56)$$

to matrix elements of the operators in Eq. (53) coupled to  $N$  external scalar fields to obtain

$$\left[ \mu \frac{d}{d\mu} - 2\tau \frac{d}{d\tau} + 2(\zeta_{\rho^2} - \gamma) \right] d_{\rho^2} = \mathcal{O}(\tau). \quad (57)$$

Here

$$\zeta_{\rho^2} = \tau \frac{d}{d\tau} \log(\mathcal{Z}_{\rho^2}(\tau, \mu^2)) \quad (58)$$

is an anomalous dimension associated with the flow-time dependence of the operator  $\rho^2(\tau, 0)$ . The renormalization group equation for the corresponding matrix element of  $\rho^2(\tau, 0)$  coupled to  $N$  external fields is given by

$$\left[ \mu \frac{d}{d\mu} - 2\tau \frac{d}{d\tau} + 2\zeta_{\rho^2} + N\gamma \right] \times \langle \Omega | \rho^2(\tau, 0) \tilde{\phi}(p_1) \dots \tilde{\phi}(p_N) | \Omega \rangle = \mathcal{O}(\tau). \quad (59)$$

We note that this equation only holds provided the flow time is small compared with the momenta of the external particles, which for DIS would be of the order of hadronic scales.

If we now demand that the smearing scale,  $\tau$ , and the inverse of the renormalization scale,  $\mu$ , are proportional to each other, i.e.,  $\tau = b/\mu^2$  with  $b$  real, then the renormalization group equation becomes

$$\left[ 2\mu \frac{d}{d\mu} + 2\zeta_{\rho^2} + N\gamma \right] \times \langle \Omega | \rho^2(b/\mu^2, 0) \tilde{\phi}(p_1) \dots \tilde{\phi}(p_N) | \Omega \rangle = \mathcal{O}(b). \quad (60)$$

This renormalization group equation provides the starting point for a nonperturbative step-scaling method [47,61] that evolves nonperturbative matrix elements to a high scale, where they can be combined with perturbative smeared Wilson coefficients. Here the renormalization group equation holds in the small flow-time limit, or, in other words, provided  $b \ll 1$ . This constraint automatically ensures that the flow time is also smaller than any hadronic length scales,  $\Lambda_{\text{QCD}} \ll \mu^2 \ll 1/\tau$ , and is generally true for

practical step-scaling methods [47,61]. We are currently investigating this approach in QCD.

## VII. CONCLUSION

We have proposed a new method, the smeared operator product expansion, to extract matrix elements from numerical nonperturbative calculations without power divergent mixing. The smeared operator product expansion is a general framework relevant to any asymptotically free theory with nonperturbative matrix elements that suffer from power divergent mixing. Within QCD, the most obvious application is to deep inelastic scattering, but other applications include nonperturbative determinations of  $K \rightarrow \pi\pi$  decays [62,63] and  $B$ -meson mixing [64]. Beyond QCD, applications include nonperturbative studies of critical phenomena in the Heisenberg model, spin systems, and other condensed matter systems.

In the sOPE, we expand nonlocal operators in a basis of smeared operators, the matrix elements of which can be determined on the lattice. We implement the smearing via the gradient flow, a classical evolution of the theory in a new dimension that smooths ultraviolet fluctuations.

The continuum limit of these matrix elements is free of power divergent mixing, provided the localization scale, the smearing length, is kept fixed in the continuum limit. The resulting matrix elements are functions of two scales, the renormalization scale and the smearing length. The sOPE systematically relates these matrix elements to smeared Wilson coefficients, which can be calculated in perturbation theory, thereby providing a complete determination of the nonlocal operators.

## ACKNOWLEDGMENTS

The authors would like to thank Martin Lüscher for helpful discussions during the course of this work and Andrea Shindler for discussions regarding related work. This project was supported in part by the U.S. Department of Energy, Grant No. DE-FG02-04ER41302. K. O. was also supported by the U.S. Department of Energy through Grant No. DE-AC05-06OR23177, under which JSA operates the Thomas Jefferson National Accelerator Facility. C. J. M. was supported in part by the U.S. National Science Foundation under Grant No. NSF PHY10-034278.

- 
- [1] J. Beringer *et al.* (Particle Data Group), *Phys. Rev. D* **86**, 010001 (2012).
  - [2] J. Collins, *Foundations of Perturbative QCD* (Cambridge University Press, Cambridge, England, 2011).
  - [3] R. Thorne and G. Watt, *J. High Energy Phys.* **08** (2011) 100.
  - [4] S. Alekhin, J. Blumlein, P. Jimenez-Delgado, S. Moch, and E. Reya, *Phys. Lett. B* **697**, 127 (2011).
  - [5] S. Alekhin, J. Blumlein, and S. Moch, *Eur. Phys. J. C* **71**, 1723 (2011).
  - [6] L. Brady, A. Accardi, W. Melnitchouk, and J. Owens, *J. High Energy Phys.* **06** (2012) 019.
  - [7] P. Jimenez-Delgado, H. Avakian, and W. Melnitchouk (Jefferson Lab Angular Momentum [JAM] Collaboration), *Phys. Lett. B* **738**, 263 (2014).
  - [8] P. Jimenez-Delgado, A. Accardi, and W. Melnitchouk, *Phys. Rev. D* **89**, 034025 (2014).
  - [9] R. D. Ball, S. Forte, A. Guffanti, E. R. Nocera, G. Ridolfi, and J. Rojo (The NNPDF Collaboration), *Nucl. Phys.* **B874**, 36 (2013).
  - [10] F. Arbabifar, A. N. Khorramian, and M. Soleymaninia, *Phys. Rev. D* **89**, 034006 (2014).
  - [11] J. Owens, A. Accardi, and W. Melnitchouk, *Phys. Rev. D* **87**, 094012 (2013).
  - [12] A. Accardi, W. Melnitchouk, J. Owens, M. Christy, C. Keppel, L. Zhu, and J. G. Morfin, *Phys. Rev. D* **84**, 014008 (2011).
  - [13] E. Leader, A. V. Sidorov, and D. B. Stamenov, *Phys. Rev. D* **82**, 114018 (2010).
  - [14] J. Blumlein and H. Bottcher, *Nucl. Phys.* **B841**, 205 (2010).
  - [15] M. Hirai and S. Kumano (Asymmetry Analysis Collaboration), *Nucl. Phys.* **B813**, 106 (2009).
  - [16] Gunnar S. Bali, S. Collins, M. Deka, B. Gläßle, M. Göckeler, J. Najjar, A. Nobile, D. Pleiter, A. Schäfer, and A. Sternbeck, *Phys. Rev. D* **86**, 054504 (2012).
  - [17] V. M. Braun *et al.* (QCDSF Collaboration), *Phys. Rev. D* **79**, 034504 (2009).
  - [18] M. Guagnelli, K. Jansen, F. Palombi, R. Petronzio, A. Shindler, and I. Wetzorke (Zeuthen-Rome [ZeRo] Collaboration), *Eur. Phys. J. C* **40**, 69 (2005).
  - [19] W. Detmold, W. Melnitchouk, and A. W. Thomas, *Mod. Phys. Lett. A* **18**, 2681 (2003).
  - [20] W. Detmold, W. Melnitchouk, and A. W. Thomas, *Eur. Phys. J. direct C* **3**, 1 (2001).
  - [21] Y.-Q. Ma and J.-W. Qiu, [arXiv:1404.6860](https://arxiv.org/abs/1404.6860).
  - [22] X. Ji, *Phys. Rev. Lett.* **110**, 262002 (2013).
  - [23] X. Ji, *Sci. China Phys. Mech. Astron.* **57**, 1407 (2014).
  - [24] H.-W. Lin, J.-W. Chen, S. D. Cohen, and X. Ji, *Phys. Rev. D* **91**, 054510 (2015).
  - [25] C. Morningstar and M. J. Peardon, *Phys. Rev. D* **69**, 054501 (2004).
  - [26] A. Hasenfratz and F. Knechtli, *Phys. Rev. D* **64**, 034504 (2001).
  - [27] C. W. Bernard and T. A. DeGrand, *Nucl. Phys. B, Proc. Suppl.* **83**, 845 (2000).
  - [28] M. Albanese *et al.*, *Phys. Lett. B* **192**, 163 (1987).
  - [29] C. Gattringer and C. B. Lang, *Quantum Chromodynamics on the Lattice* (Springer, Berlin, 2010).
  - [30] M. Lüscher, *J. High Energy Phys.* **04** (2013) 123.

- [31] M. Lüscher and P. Weisz, *J. High Energy Phys.* **02** (2011) 051.
- [32] M. Lüscher, *J. High Energy Phys.* **08** (2010) 071.
- [33] R. Narayanan and H. Neuberger, *J. High Energy Phys.* **03** (2006) 064.
- [34] R. Lohmayer and H. Neuberger, *Proc. Sci.*, LATTICE 2011, 249 (2011).
- [35] H. Makino and H. Suzuki, *Prog. Theor. Exp. Phys.* **2015**, 33B08 (2015).
- [36] Z. Davoudi and M. J. Savage, *Phys. Rev. D* **86**, 054505 (2012).
- [37] S. Borsanyi, S. Durr, Z. Fodor, S. D. Katz, S. Krieg, T. Kurth, S. Mages, A. Schafer, and K. K. Szabo, [arXiv: 1205.0781](https://arxiv.org/abs/1205.0781).
- [38] S. Borsanyi, S. Durr, Z. Fodor, C. Hoelbling, S. D. Katz, T. Kurth, L. Lellouch, T. Lippert, and C. McNeile, *J. High Energy Phys.* **09** (2012) 010.
- [39] A. Bazavov *et al.* (MILC Collaboration), *Proc. Sci.*, LATTICE 2013, 269 (2013).
- [40] Z. Fodor, K. Holland, J. Kuti, S. Mondal, D. Nogradi, and C. H. Wong, *J. High Energy Phys.* **09** (2014) 018.
- [41] A. Cheng, A. Hasenfratz, Y. Liu, G. Petropoulos, and D. Schaich, *J. High Energy Phys.* **05** (2014) 137.
- [42] Z. Fodor, K. Holland, J. Kuti, D. Nogradi, and C. H. Wong, *J. High Energy Phys.* **11** (2012) 007.
- [43] P. Fritzsche, A. Ramos, and F. Stollenwerk, *Proc. Sci.*, LATTICE 2013, 461 (2013).
- [44] P. Fritzsche and A. Ramos, *Proc. Sci.*, LATTICE 2013, 319 (2013).
- [45] A. Ramos, *Proc. Sci.*, LATTICE 2013, 053 (2013).
- [46] J. Rantaharju, *Proc. Sci.*, LATTICE 2013, 084 (2013).
- [47] C. Monahan and K. Orginos, *Proc. Sci.*, LATTICE 2013, 443 (2013).
- [48] M. Lüscher, *J. High Energy Phys.* **06** (2014) 105.
- [49] A. Shindler, *Nucl. Phys.* **B881**, 71 (2014).
- [50] H. Suzuki, *Prog. Theor. Exp. Phys.* **2013**, 83B03 (2013).
- [51] L. Del Debbio, A. Patella, and A. Rago, *J. High Energy Phys.* **11** (2013) 212.
- [52] H. Makino and H. Suzuki, *Prog. Theor. Exp. Phys.* **2014**, 63B02 (2014).
- [53] J. Collins, *Renormalization: An Introduction to Renormalization, the Renormalization Group and the Operator-Product Expansion* (Cambridge University Press, Cambridge, England, 1984).
- [54] C. Bonati and M. D'Elia, *Phys. Rev. D* **89**, 105005 (2014).
- [55] M. Asakawa, T. Hatsuda, E. Itou, M. Kitazawa, and H. Suzuki (FlowQCD Collaboration), *Phys. Rev. D* **90**, 011501 (2014).
- [56] S. Hollands and C. Kopper, *Commun. Math. Phys.* **313**, 257 (2012).
- [57] C. Monahan, *Proc. Sci.*, LATTICE 2013, 021 (2013).
- [58] S. Capitani, *Phys. Rep.* **382**, 113 (2003).
- [59] H. Kleinert and V. Schulte-Frohlinde, *Critical Properties of  $\phi^4$ -Theories* (World Scientific, Singapore, 2001).
- [60] S. E. Derkachov, J. Gracey, and A. Manashov, *Eur. Phys. J. C* **2**, 569 (1998).
- [61] M. Lüscher, P. Weisz, and U. Wolff, *Nucl. Phys.* **B359**, 221 (1991).
- [62] C. Dawson, G. Martinelli, G. Rossi, C. T. Sachrajda, S. R. Sharpe, M. Talevi, and M. Testa, *Nucl. Phys.* **B514**, 313 (1998).
- [63] W. Detmold and C. D. Lin, *Phys. Rev. D* **73**, 014501 (2006).
- [64] C. Monahan, E. Gamiz, R. Horgan, and J. Shigemitsu, *Phys. Rev. D* **90**, 054015 (2014).